

Anomalous thermal conductivity and magnetic torque response in the honeycomb magnet α -RuCl₃

Ian A. Leahy,¹ Christopher A. Pocs,¹ Peter E. Siegfried,¹ David Graf,²
S.-H. Do,³ Kwang-Yong Choi,³ B. Normand,⁴ and Minhyea Lee¹

¹*Department of Physics, University of Colorado, Boulder, CO 80309, USA*

²*National High Magnetic Field Laboratory, Tallahassee, FL 32310, USA*

³*Department of Physics, Chung-Ang University, Seoul, 790-784, South Korea*

⁴*Laboratory for Neutron Scattering and Imaging,*

Paul Scherrer Institute, CH-5232 Villigen PSI, Switzerland

(Dated: March 10, 2017)

We report on the unusual behavior of the in-plane thermal conductivity (κ) and torque (τ) response in the Kitaev-Heisenberg material α -RuCl₃. κ shows a striking enhancement with linear growth beyond $H = 7$ T, where magnetic order disappears, while τ for both of the in-plane symmetry directions shows an anomaly at the same field. The temperature- and field-dependence of κ are far more complex than conventional phonon and magnon contributions, and require us to invoke the presence of unconventional spin excitations whose properties are characteristic of a field-induced spin-liquid phase related to the enigmatic physics of the Kitaev model in an applied magnetic field.

PACS numbers:

Low-dimensional spin systems display a multitude of quantum phenomena, providing an excellent forum for the exploration of unconventional ground states and their exotic excitations. The Kitaev model [1] has attracted particular attention, both theoretically and experimentally, because it possesses an exactly solvable quantum spin-liquid (QSL) ground state and has possible realizations in a number of candidate materials [2–5]. Thermal transport measurements have proven to be a powerful tool for elucidating the itinerant nature of QSLs [6, 7], as a result of their high sensitivity to the low-energy excitation spectrum, and in fact studies of low-dimensional insulating quantum magnets have revealed very significant contributions to heat conduction from unconventional spin excitations [8–18].

Magnetic insulators containing $4d$ and $5d$ elements combine electronic correlation effects with strong spin-orbit coupling (SOC) to generate complex magnetic interactions. In the Kitaev model, nearest-neighbor spin- $\frac{1}{2}$ entities on a two-dimensional (2D) honeycomb lattice interact through a bond-dependent Ising-type coupling of different spin components, whose strong frustration leads to a QSL ground state with emergent gapless and gapped Majorana-fermion excitations [1]. The physical realization of this uniquely anisotropic interaction requires strong SOC, which creates effective $j_{\text{eff}} = \frac{1}{2}$ moments with Kitaev-type coupling in the honeycomb iridate compounds A₂IrO₃ (A = Na or Li) [19, 20]. Despite its weaker SOC, the $4d$ honeycomb material α -RuCl₃ contains similar spin-orbit-entangled moments, and thus has emerged as another candidate system for Kitaev-related physics [5, 21–23].

In this Letter, we present in-plane thermal conductivity (κ) and magnetic torque (τ) studies of single-crystal α -RuCl₃ samples. Below the magnetic ordering temper-

ature, T_C , a pronounced minimum of κ and an accompanying torque anomaly at $H = H_{\text{min}} \simeq 7$ T occur due to a field-induced phase transition from the “zig-zag” ordered state [21, 24] to a spin-disordered phase. The abrupt and linear rise of the low- T κ at $H > H_{\text{min}}$ indicates that this field-induced spin liquid (FISL) contains a massless excitation with Dirac-type dispersion, while the strong renormalization of the phonon contribution at all temperatures suggests a broad band of unconventional medium-energy excitations. These results serve to fingerprint the possible Kitaev physics of the FISL in α -RuCl₃.

Single crystals of RuCl₃ were synthesized by vacuum sublimation [25], as described in Sec. SI of the Supplementary Material (SM) [26]. κ measurements were performed with a one-heater, two-thermometer configuration in a ³He refrigerator and external magnetic fields up to 14 T. Cernox and RuO_x resistors were used as thermometers for the respective temperature ranges $T > 2$ K and $0.3 < T \leq 15$ K, and were calibrated both separately and in-situ under the applied field. Both the thermal current ($-\nabla T$) and the field were oriented in the crystalline ab -plane, with H applied either parallel or perpendicular to ∇T . We found little difference in κ for the two orientations, and all results shown below were measured in the $\nabla T \parallel H \parallel ab$ geometry, other than Fig. 1(b), where $\nabla T \perp H$. τ was determined from capacitance measurements between the ground plane and a BeCu cantilever. Its angular dependence was measured in two geometries, one in which H was rotated within the ab -plane (ϕ rotation) and one with H rotated out of plane (θ rotation).

Figure 1(a) shows $\kappa(T)$, in fields $\mu_0 H = 0$ and 14 T, for three α -RuCl₃ samples. Qualitatively, the dependence of κ on both T and H is the same in each case, and we focus on these general features. Quantitatively, our samples show differences in peak heights and

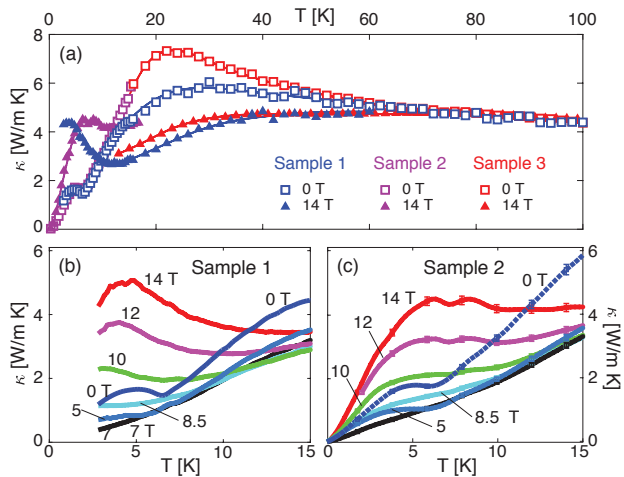


FIG. 1: (a) In-plane thermal conductivity, $\kappa(T)$, shown up to 100 K for Samples 1, 2, and 3 at $\mu_0 H = 0$ T (squares) and 14 T (triangles). Solid lines are a guide to the eye. (b) Low-temperature detail of $\kappa(T)$ for a range of H values, shown for Sample 1. (c) $\kappa(T)$ at low T for Sample 2.

widths, which we relate to their age and defect content in Sec. SI of the SM [26]. On cooling at zero field (ZF), $\kappa_0(T) = \kappa(T, H = 0)$ has a broad peak near 25 K and decreases down to the magnetic ordering temperature, $T_C \simeq 6.3$ K, which is identified both from the upturn in κ and from the magnetic susceptibility (data not shown). This value of T_C is identified clearly in all our crystals, testifying to their high as-grown quality, with no contamination from structures of different layer stackings [27]. For $T < T_C$, $\kappa_0(T)$ shows a weak maximum before decreasing to zero. $\kappa(T, 14$ T) differs dramatically from $\kappa_0(T)$ at all temperatures below 60 K. Its peak at intermediate T is suppressed, broader, and lies at a higher temperature, whereas below $T \simeq 12$ K it has a strong low- T peak that is completely absent from $\kappa_0(T)$.

Focusing on this low- T regime, Figs. 1(b) and 1(c) show $\kappa(T)$ at constant fields $H = 0, 5, 7, 8.5, 10, 12$, and 14 T. Because the ordered state has a large magnon gap [28], the weak low- T , low- H feature is in fact an enhanced phonon contribution. This is suppressed by increasing field, and the minimum marking T_C is visible up to $H = 5$ T. At $H = H_{\min} \simeq 7$ T, both the phonon enhancement and the minimum disappear. Further increase of H causes the appearance of the low- T peak, whose height grows linearly with $H - H_{\min}$, leading to rounded maxima around 5 K at 14 T. We have collected detailed low- T data ($0.3 < T < 3$ K) at $H > H_{\min}$ for Sample 2 [Fig. 1(c)] and find that these do not display an activated form; the alternative of a power-law form demonstrates clearly that this feature is the contribution of a gapless excitation.

The non-monotonic evolution with H and the strong high-field enhancement of κ are clearly evident in the

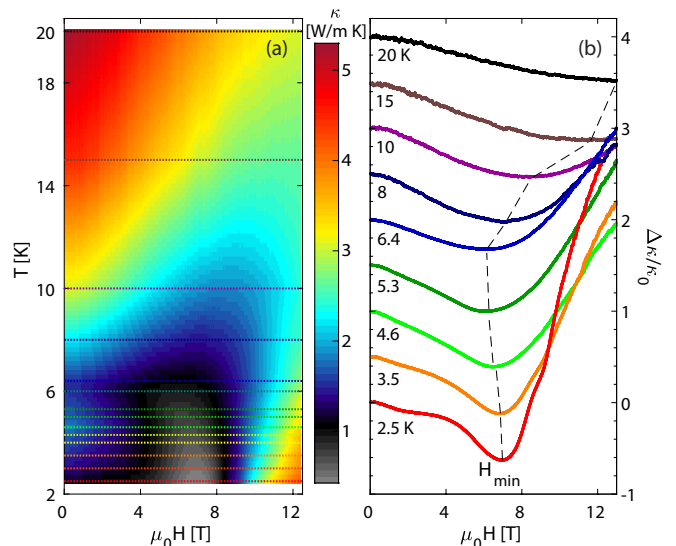


FIG. 2: (a) $\kappa(T, H)$ for Sample 1, represented by color contours. Horizontal lines correspond to field sweeps measuring $\kappa(H)$ at fixed T . (b) Relative thermal conductivity difference, $\Delta\kappa(H)/\kappa_0$, shown for the fixed values of T highlighted in panel (a); curves are presented with constant offsets.

isothermal H -dependence. Figure 2(a) presents $\kappa(H, T)$ for Sample 1 as a color contour map, showing the minimum region around H_{\min} and maxima at high T or high H . The fractional change of $\kappa(H)$, $\Delta\kappa(H)/\kappa_0 = (\kappa(H) - \kappa_0)/\kappa_0$, is shown in Fig. 2(b) for a range of T values. $\kappa(H)$ and $\Delta\kappa(H)/\kappa_0$ show an initial decrease, before turning over at H_{\min} and increasing rapidly. $H_{\min}(T)$ remains around 7 T for $T < T_C$, but becomes rapidly larger as T is increased beyond T_C , making the minima shallower until at $T = 20$ K H_{\min} is pushed outside our measurement range. Our measured value $H_{\min} \simeq 7$ T for $T < 10$ K coincides with the critical field (H_C) for the field-induced phase transition observed in bulk magnetization [24] and specific-heat measurements [29]. Further, the magnetization in this field range is far from saturation [24, 29] and it is safe to conclude that the system is only weakly spin-polarized above H_{\min} .

In general, κ contains multiple terms whose effects can be difficult to separate. For α - RuCl_3 , the presence and location of H_{\min} are fundamental properties of the phase diagram and four further, distinctive features provide clues about the primary contributions to κ . These are (i) the local minimum in $\kappa(T)$ occurring at T_C at small H [Figs. 1(b) and 1(c)], (ii) the slow decrease of $\kappa(H)$ when H increases from zero [Fig. 2(b)], (iii) the properties of the low- T peak in $\kappa(T)$ at $H > H_{\min}$ [Figs. 1(b) and 1(c)], and (iv) the suppression and shift of the intermediate-temperature contribution by the applied field [Fig. 1(a)].

Features (i) and (ii) can be explained within a conventional framework. The magnetic anisotropy of RuCl_3 re-

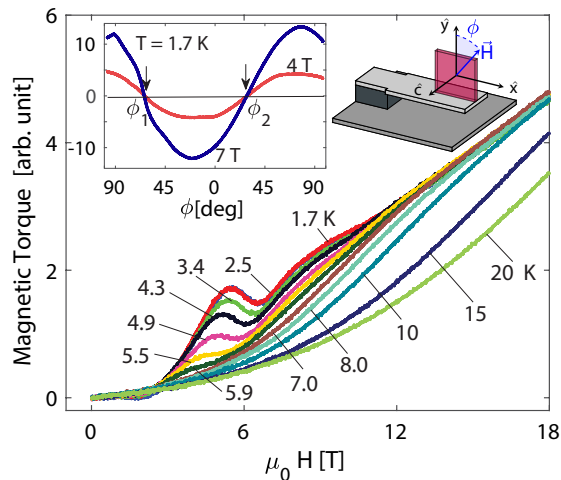


FIG. 3: In-plane torque response as a function of H , measured at selected values of T with $\phi = -69 \pm 2^\circ$. Right inset: measurement configuration. Left inset: ϕ -dependence of τ at fields of 4 T and 7 T; $\phi_1 = -64^\circ$ and $\phi_2 = 28^\circ$ exhibit 90° symmetry ($\phi = 0^\circ$ is chosen arbitrarily).

sults in a magnon gap of 1.7 meV [28] in the ordered state, and thus no spin-wave contribution can be expected. In many systems, κ decreases rapidly below the Curie-Weiss temperature, T_{CW} , due to the scattering of phonons by spin fluctuations, which reduces the phonon mean free path, l_p . Such spin-phonon scattering is thought to have a strong impact on the phonon contribution to heat conduction in SOC materials [30, 31]. In RuCl_3 , this effect is visible below $T_{CW} \approx 25$ K [21] at ZF [Fig. 1(a)]. However, spin fluctuations are suppressed due to the onset of magnetic order, i.e. below $T = T_C$. Thus the weak low- T , low- H feature, whose vanishing causes the pronounced local minimum at T_C in ZF (i), is caused by the enhancement of κ expected from the improved l_p . By the same token, the weak decrease of κ with T for $H < H_{\min}$ (ii) is a consequence of the applied field suppressing the magnetic order, and with it the improved l_p .

Before discussing features (iii) and (iv), for further perspective concerning the phases below and above H_{\min} we have performed magnetic torque measurements on our RuCl_3 single crystals. We rotate H both within the ab -plane (Fig. 3, right inset) and out of it [discussed in Sec. SII of the SM [26]]. The torque generated in the presence of a magnetization, M , is $\vec{\tau} = \mu_0 \mathbf{M} \mathbf{V} \times \mathbf{H}$, with μ_0 the permeability and V the sample volume. The thermodynamic quantity τ is highly sensitive to magnetic anisotropy [32, 33]. Measurements performed on three crystals, of different shapes and sizes, all returned results very similar to those shown in Fig. 3.

In the ab -plane, $\tau(\phi)$ displays the 90° symmetry expected due to the monoclinic structure of $\alpha\text{-RuCl}_3$ [25, 27] (Fig. 3, left inset). At two specific angles, ϕ_1 and ϕ_2 ,

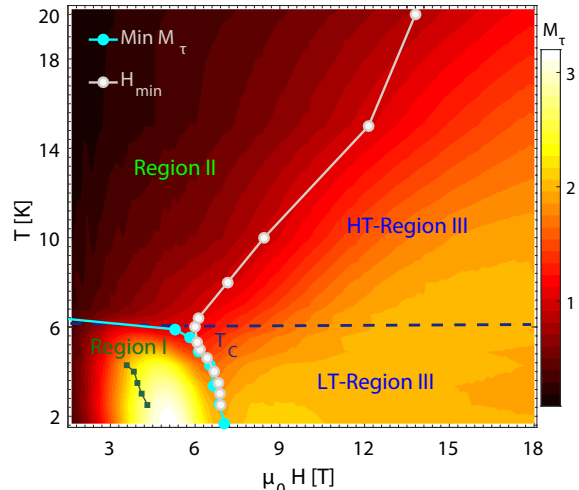


FIG. 4: (a) (H, T) phase diagram of $\alpha\text{-RuCl}_3$ inferred from the magnitude of M_τ measured at $\phi \simeq -69^\circ$ (color scale). White circles indicate H_{\min} as a function of T , cyan circles the position of local minima in $M_\tau(H)$, and green squares the locations of inflection points appearing in $\Delta\kappa/\kappa_0(H)$ [Fig. 2(b)].

$\tau \rightarrow 0$ independent of the magnitude of H , and Fig. 3 shows $\tau(H)$ measured near ϕ_1 (results near ϕ_2 are qualitatively similar). At low T , $\tau(H)$ with $H < H_{\min}$ exhibits a strikingly non-monotonic form. This complexity ceases abruptly at $H > H_{\min}$. At $T > T_C$, the sizes both of τ and of the anomaly drop significantly, indicating strongly that this behavior is due solely to the presence of magnetic order. Such anomalous H -dependence is not surprising in a Hamiltonian as anisotropic as the Kitaev-Heisenberg model, and a rich variety of complex field-induced ordering patterns, with corresponding off-diagonal components of the magnetic susceptibility tensor, has been suggested [34, 35].

We define the torque magnetization, $M_\tau = \tau/H$, which in certain geometries is closely related to the real magnetization (as discussed in Sec. III of the SM [26]). Figure 4 shows $M_\tau(H, T)$ in the form of color contours [36]. The overlaid points showing the characteristic quantities $H_{\min}(T)$ and the minima of M_τ divide this effective H - T phase diagram naturally into three distinct regions. Region I, at $T < T_C$ and $H < H_{\min}$, is where spontaneous magnetic order exists and is characterized by the strongly non-monotonic $\tau(H)$ and decreasing $\kappa(H)$ ($d\kappa/dH < 0$). Here also the inflection points of $\kappa(H)$ at $H < H_{\min}$ [Fig. 4(a)] coincide with the local maxima of τ (Fig. 3). In Region II, $d\kappa/dH < 0$ while $T > T_C$. Region III is characterized by $d\kappa/dH > 0$, but the derivative falls rapidly as T crosses T_C , leading us to divide it into LT-Region III ($T < T_C$), where we observe the strongest enhancement of $\Delta\kappa/\kappa_0$, and HT-Region III ($T > T_C$), where H_{\min} moves rapidly to higher values.

Features (iii) and (iv) in κ are respectively the key properties of Regions LT–III and HT–III. Before invoking exotic physics, the conventional explanations should be exhausted. Modelling all the contributions of phonons and coherent spin excitations to κ is a complicated problem [8–15, 17, 18]. The first complexity for α -RuCl₃ is the quasi-2D structure, which would require a currently unavailable anisotropic 3D phonon fit. Conventional phonon thermal conductivity in a magnetic insulator is ascribed to four contributions, point defects, grain boundaries, Umklapp processes, and magnon-phonon resonant scattering [37–39]. The last has been used successfully to describe the H -dependence of features observed in κ in several low-dimensional materials [10, 40, 41]. However, its effect is usually to generate a minimum at the resonance energy, causing a double-peak structure in $\kappa(T)$ where only the lower peak has strong H -dependence [8, 10, 41]. Such behavior is qualitatively different from α -RuCl₃, and in fact we are not aware of a mechanism for a strong field-induced enhancement of κ , of the type we observe in Figs. 1(b) and 1(c), other than a coherent spin excitation [12–14, 16, 42]. However, α -RuCl₃ at $H > H_{\min}$ has no magnetic order, as demonstrated by the absence of features in the susceptibility [21] and specific heat [29], and verified by neutron scattering [43] and nuclear magnetic resonance studies [44]. Thus it has no conventional gapless mode, and this is why we conclude that feature (iii) must attributed to an unconventional excitation of the FISL.

Turning to exotic solutions, the proximity of the zig-zag ordered state to a Kitaev QSL at ZF [22] is strongly suggestive. However, we note that an applied field destroys many of the exotic properties of the Kitaev QSL [1], that the FISL is partially spin-polarized, that the Heisenberg terms have non-trivial effects [22], and that ideal honeycomb symmetry is broken in monoclinic α -RuCl₃ [27, 45]. It is nevertheless instructive to recall that the Kitaev model has an exact solution in terms of Majorana fermions, one of which is massless with linear dispersion [1] while the others are massive. Spin excitations are Majorana pairs, or equivalently Majorana modes pinned to static fluxes [46], and are all massive. Although one recent numerical study reports a QSL state above a critical field in a model for RuCl₃ [47], it was found to be gapped. The low- and medium-energy spin excitations of RuCl₃ at ZF have been mapped by recent inelastic neutron scattering studies [28, 48]. In addition to the gapped spin waves, one finds a broad continuum of excitations centered around 5 meV [48]. At finite fields, no information is yet available, other than the κ signals we measure. In this context it is of crucial importance that the low- T excitations contributing above H_{\min} are gapless and that their density of states, measured by κ , increases linearly with H [feature (iii)]. These are the properties of a cone-type dispersion and are thus the same behavior as the massless Kitaev QSL mode.

Feature (iv) is the striking field-dependence of $\kappa(T)$ for $T_C < T < 60$ K [Fig. 1(a)]. In this range κ should be dominated by phonons, whose contributions are H -independent. The presence of an incoherent medium-energy continuum of anisotropic spin excitations [48] may cause a direct contribution to κ or a suppression due to spin-phonon scattering. Our results contain no evidence for direct contributions, as there is no abrupt change in κ at H_{\min} and the change in the high- T peak position indicates energy shifts far beyond the scale of H . By contrast, our results contain several features characterizing a strong suppression of phonon contributions. First, κ at ZF cannot be fitted within the conventional framework, indicating that anomalous phonon scattering is significant even at $H = 0$. Second, the continuum affects the phonon contributions to κ over a broad range of T [Fig. 1(a)], reflecting the broad energy range observed in Ref. [48]. Third, scattering becomes considerably more effective at a field of 14 T. Because the field scale for a significant reconstruction of the continuum should be the Kitaev energy, estimated as $K \approx 7$ meV [23, 28], it is clear that some rearrangement must take place at the field-induced transition to the FISL. However, the lack of abrupt changes in κ at H_{\min} indicates that only a small fraction of the continuum turns into the massless mode [feature (iii)], while the majority of its spectral weight remains in a broad continuum at finite energies; we comment here that thermal fluctuations may cause at least as strong a rearrangement of the continuum over the T range of our experiment as field effects do. Thus from the evidence provided by $\kappa(H, T)$, the FISL does appear to possess both the primary excitation features of the Kitaev QSL, namely a Dirac-type band and a finite-energy continuum. For this reason we refer to them as proximate Kitaev excitations (PKEs).

To summarize the nature of heat conduction in α -RuCl₃ in the context of Fig. 4, κ in Region I is controlled by low- T phonon contributions, decreasing slowly as the system is driven towards the FISL because l_p is reduced. A similar trend continues in Region II, where the increasing thermal population of phonons, as well as thermally excited paramagnons, contribute to κ . In LT–Region III, the rapid increase of κ with H reflects the presence of the massless PKE. In HT–Region III, the minimum of $\kappa(H)$ moves to high fields (Fig. 4) and there are contributions to κ both from phonons and from the massive PKEs, where the primary effect of the latter is the systematic suppression of the former with increasing H , which drives up the crossover field [$H_{\min}(T)$] from Region II.

To conclude, we have investigated the highly non-monotonic thermal conductivity and the torque magnetization response of the 2D honeycomb-lattice material RuCl₃. We infer a field-induced phase transition to a state, the FISL, of no magnetic order and no simple spin polarization. The low-energy excitations of this spin-disordered ground state cause a dramatic enhancement of

κ at low temperatures, while its gapped excitations suppress the phonon contribution at higher temperatures, and do so more effectively at higher fields. Although our results neither prove nor disprove that the FISL is closely related to the Kitaev QSL state, they set strong constraints on the nature of its excitations and thus of its theoretical description.

Acknowledgment We thank A. Chernyshev and M. Hermele for helpful discussions. This work was supported by the US DOE, Basic Energy Sciences, Materials Sciences and Engineering Division, under Award Number de-sc0006888. Torque magnetometry was performed at the National High Magnetic Field Laboratory, which is supported by National Science Foundation Cooperative Agreement No. DMR-1157490 and the State of Florida.

-
- [1] A. Kitaev, *Ann. Phys.* **321**, 2 (2006).
- [2] G. Jackeli and G. Khaliullin, *Phys. Rev. Lett.* **102**, 017205 (2009), URL <http://link.aps.org/doi/10.1103/PhysRevLett.102.017205>.
- [3] J. Chaloupka, G. Jackeli, and G. Khaliullin, *Phys. Rev. Lett.* **105**, 027204 (2010), URL <http://link.aps.org/doi/10.1103/PhysRevLett.105.027204>.
- [4] Y. Singh, S. Manni, J. Reuther, T. Berlijn, R. Thomale, W. Ku, S. Trebst, and P. Gegenwart, *Phys. Rev. Lett.* **108**, 127203 (2012), URL <http://link.aps.org/doi/10.1103/PhysRevLett.108.127203>.
- [5] K. W. Plumb, J. P. Clancy, L. J. Sandilands, V. V. Shankar, Y. F. Hu, K. S. Burch, H.-Y. Kee, and Y.-J. Kim, *Phys. Rev. B* **90**, 041112 (2014), URL <http://link.aps.org/doi/10.1103/PhysRevB.90.041112>.
- [6] M. Yamashita, N. Nakata, Y. Kasahara, T. Sasaki, N. Yoneyama, N. Kobayashi, S. Fujimoto, T. Shibauchi, and Y. Matsuda, *Nature Phys.* **5**, 44 (2008).
- [7] M. Yamashita, N. Nakata, Y. Senshu, M. Nagata, H. M. Yamamoto, R. Kato, T. Shibauchi, and Y. Matsuda, *Science* **328**, 1246 (2010), URL <http://science.sciencemag.org/content/328/5983/1246>.
- [8] Y. Ando, J. Takeya, D. L. Sisson, S. G. Doettinger, I. Tanaka, R. S. Feigelson, and A. Kapitulnik, *Phys. Rev. B* **58**, R2913 (1998), URL <http://link.aps.org/doi/10.1103/PhysRevB.58.R2913>.
- [9] A. V. Sologubenko, K. Giannó, H. R. Ott, U. Ammerahl, and A. Revcolevschi, *Phys. Rev. Lett.* **84**, 2714 (2000), URL <http://link.aps.org/doi/10.1103/PhysRevLett.84.2714>.
- [10] M. Hofmann, T. Lorenz, G. S. Uhrig, H. Kierspel, O. Zabara, A. Freimuth, H. Kageyama, and Y. Ueda, *Phys. Rev. Lett.* **87**, 047202 (2001), URL <http://link.aps.org/doi/10.1103/PhysRevLett.87.047202>.
- [11] A. V. Sologubenko, K. Gianno, H. R. Ott, A. Vietkine, and A. Revcolevschi, *Physical Review B* **64**, 054412 (2001).
- [12] B. C. Sales, M. D. Lumsden, S. E. Nagler, D. Mandrus, and R. Jin, *Phys. Rev. Lett.* **88**, 095901 (2002), URL <http://link.aps.org/doi/10.1103/PhysRevLett.88.095901>.
- [13] R. Jin, Y. Onose, Y. Tokura, D. Mandrus, P. Dai, and B. C. Sales, *Phys. Rev. Lett.* **91**, 146601 (2003), URL <http://link.aps.org/doi/10.1103/PhysRevLett.91.146601>.
- [14] S. Y. Li, L. Taillefer, C. H. Wang, and X. H. Chen, *Phys. Rev. Lett.* **95**, 156603 (2005), URL <http://link.aps.org/doi/10.1103/PhysRevLett.95.156603>.
- [15] C. Hess, *Eur. Phys. J. Special Topics* **151**, 73 (2007).
- [16] X. F. Sun, W. Tao, X. M. Wang, and C. Fan, *Phys. Rev. Lett.* **102**, 167202 (2009), URL <http://link.aps.org/doi/10.1103/PhysRevLett.102.167202>.
- [17] L. M. Chen, X. M. Wang, W. P. Ke, Z. Y. Zhao, X. G. Liu, C. Fan, Q. J. Li, X. Zhao, and X. F. Sun, *Phys. Rev. B* **84**, 134429 (2011), URL <http://link.aps.org/doi/10.1103/PhysRevB.84.134429>.
- [18] A. Mohan, N. S. Beesetty, N. Hlubek, R. Saint-Martin, A. Revcolevschi, B. Büchner, and C. Hess, *Phys. Rev. B* **89**, 104302 (2014), URL <http://link.aps.org/doi/10.1103/PhysRevB.89.104302>.
- [19] S. K. Choi, R. Coldea, A. N. Kolmogorov, T. Lancaster, I. I. Mazin, S. J. Blundell, P. G. Radaelli, Y. Singh, P. Gegenwart, K. R. Choi, S.-W. Cheng, P. J. Baker, C. Stock, J. Taylor, *Phys. Rev. Lett.* **108**, 127204 (2012), URL <http://link.aps.org/doi/10.1103/PhysRevLett.108.127204>.
- [20] S. H. Chun, J.-W. Kim, J. Kim, H. Zheng, C. C. Stoumpos, C. D. Malliakas, J. F. Mitchell, K. Mehlawat, Y. Singh, Y. Choi, T. Gog, A. Al-Zein, M. Sala, M. Krisch, J. Chaloupka, G. Jackeli, G. Khaliullin, B. J. Kim, *Nature Physics* **11**, 462 (2015).
- [21] J. A. Sears, M. Songvilay, K. W. Plumb, J. P. Clancy, Y. Qiu, Y. Zhao, D. Parshall, and Y.-J. Kim, *Phys. Rev. B* **91**, 144420 (2015), URL <http://link.aps.org/doi/10.1103/PhysRevB.91.144420>.
- [22] J. G. Rau, E. K.-H. Lee, and H.-Y. Kee, *Phys. Rev. Lett.* **112**, 077204 (2014), URL <http://link.aps.org/doi/10.1103/PhysRevLett.112.077204>.
- [23] H.-S. Kim, V. V. Shankar, A. Catuneanu, and H.-Y. Kee, *Phys. Rev. B* **91**, 241110 (2015), URL <http://link.aps.org/doi/10.1103/PhysRevB.91.241110>.
- [24] R. D. Johnson, S. C. Williams, A. A. Haghighirad, J. Singleton, V. Zapf, P. Manuel, I. I. Mazin, Y. Li, H. O. Jeschke, R. Valentí, and R. Coldea, *Phys. Rev. B* **92**, 235119 (2015), URL <http://link.aps.org/doi/10.1103/PhysRevB.92.235119>.
- [25] S.-Y. Park, S.-H. Do, K.-Y. Choi, D. Jang, T.-H. Jang, J. Schefer, C.-M. Wu, J. S. Gardner, J. M. S. Park, J.-H. Park, and S. Ji, arXiv:1609.05690.
- [26] For details see the Supplementary Material at [url].
- [27] H. B. Cao, A. Banerjee, J.-Q. Yan, C. A. Bridges, M. D. Lumsden, D. G. Mandrus, D. A. Tennant, B. C. Chakoumakos, and S. E. Nagler, *Phys. Rev. B* **93**, 134423 (2016), URL <http://link.aps.org/doi/10.1103/PhysRevB.93.134423>.
- [28] A. Banerjee, C. A. Bridges, J.-Q. Yan, A. A. Aczel, L. Li, M. B. Stone, G. E. Granroth, M. D. Lumsden, Y. Yiu, J. Knolle, D. L. Kovrizhin, S. Bhattacharjee, D. A. Tennant, R. Moessner, D. G. Mandrus, and S. E. Nagler, *Nature Mater.* **15**, 733 (2016).
- [29] Y. Kubota, H. Tanaka, T. Ono, Y. Narumi, and K. Kindo, *Phys. Rev. B* **91**, 094422 (2015), URL <http://link.aps.org/doi/10.1103/PhysRevB.91.094422>.
- [30] F. Steckel, A. Matsumoto, T. Takayama, H. Takagi, B. Büchner, and C. Hess, *Eur. Phys. Lett.* **114**, 57007 (2016), URL <http://stacks.iop.org/0295-5075/114/>

- i=5/a=57007.
- [31] A. L. Chernyshev, Phys. Rev. B **72**, 174414 (2005), URL <http://link.aps.org/doi/10.1103/PhysRevB.72.174414>.
- [32] R. Okazaki, T. Shibauchi, H. J. Shi, Y. Haga, T. D. Matsuda, E. Yamamoto, Y. Onuki, H. Ikeda, and Y. Matsuda, Science **331**, 439 (2011), URL <http://science.sciencemag.org/content/331/6016/439>.
- [33] S. Kasahara, H. J. Shi, K. Hashimoto, S. Tonegawa, Y. Mizukami, T. Shibauchi, K. Sugimoto, T. Fukuda, T. Terashima, A. H. Nevidomskyy, and Y. Matsuda, Nature **486**, 382 (2012).
- [34] L. Janssen, E. C. Andrade, and M. Vojta, Phys. Rev. Lett. **117**, 277202 (2016).
- [35] G.-W. Chern, Y. Sizyuk, C. Price, and N. B. Perkins, arXiv:1611.03436.
- [36] Figure S3 of the SM shows the corresponding curves for $M_r(H)$ at different values of T [26].
- [37] P. Klemens, *Solid State Physics Vol. 7* (Academic Press, New York, 1958).
- [38] J. Callaway, Phys. Rev. **113**, 1046 (1959), URL <http://link.aps.org/doi/10.1103/PhysRev.113.1046>.
- [39] R. Bergman, *Thermal conduction in solids* (Oxford University Press, Oxford, 1979).
- [40] J. C. Wu, J. D. Song, Z. Y. Zhao, J. Shi, H. S. Xu, J. Y. Zhao, X. G. Liu, X. Zhao, and X. F. Sun, J. Phys.: Condens. Matter **28**, 056002 (2016), URL <http://stacks.iop.org/0953-8984/28/i=5/a=056002>.
- [41] B.-G. Jeon, B. Koteswararao, C. B. Park, G. J. Shu, S. C. Riggs, E. G. Moon, S. B. Chung, F. C. Chou, and K. H. Kim, Sci. Rep. **6**, 36970 (2010), URL <http://dx.doi.org/10.1038/srep36970>.
- [42] X. M. Wang, C. Fan, Z. Y. Zhao, W. Tao, X. G. Liu, W. P. Ke, X. Zhao, and X. F. Sun, Phys. Rev. B **82**, 094405 (2010), URL <http://link.aps.org/doi/10.1103/PhysRevB.82.094405>.
- [43] S. E. Nagler, private communication.
- [44] S.-H. Baek, S.-H. Do, K.-Y. Choi, Y. S. Kwon, A. U. B. Wolter, J. van den Brink, and B. Büchner, arXiv:1702.01671.
- [45] H.-S. Kim and H.-Y. Kee, Phys. Rev. B **93**, 155143 (2016), URL <http://link.aps.org/doi/10.1103/PhysRevB.93.155143>.
- [46] G. Baskaran, S. Mandal, and R. Shankar, Phys. Rev. Lett. **98**, 247201 (2007).
- [47] R. Yadav, N. A. Bogdanov, V. M. Katukuri, S. Nishimoto, J. van den Brink, and L. Hozoi, Sci. Rep. **6**, 37925 (2016).
- [48] A. Banerjee, J.-Q. Yan, J. Knolle, C. A. Bridges, M. B. Stone, M. D. Lumsden, D. G. Mandrus, D. A. Tennant, R. Moessner, and S. E. Nagler, arXiv:1609.00103.

Supplemental Material

Anomalous thermal conductivity and magnetic torque response in the honeycomb magnet α -RuCl₃

Ian A. Leahy, Christopher A. Pocs, Peter E. Siegfried, David Graf, S.-H. Do, Kwang-Yong Choi, B. Normand, and Minhyea Lee

SI. Sample Synthesis and Sample-Dependence

Sample Synthesis

The α -RuCl₃ single crystals used in this study were grown by a vacuum sublimation method. A commercial RuCl₃ powder (Alfa-Aesar), which consists of β -RuCl₃ with a small fraction of RuO₂ and RuOCl₂, was ground thoroughly and dehydrated in an evacuated quartz ampoule. When the sealed ampoule is heated at 600°C for one day, the β -phase of RuCl₃ undergoes a transition to the α -phase, while RuOCl₂ decomposes to RuO₂, α -RuCl₃, and Cl₂ gas. The remaining RuO₂ in the mixture intervenes in the α -RuCl₃ powder phase. During the course of crystallization, single crystals of RuO₂ grow separately from the α -RuCl₃ crystals, allowing their removal by mechanical treatment, and thus no additional purification was required. The ampoule was placed in a temperature-gradient furnace for vapor transport. The mixture was heated to 1080°C, then cooled to 650°C at a rate of -2°C per hour. We obtain pieces of α -RuCl₃ single crystals at the end of the ampoule. Single-crystal diffraction and EDX (Electron Dispersive X-ray) mea-

surements confirm that these α -RuCl₃ crystals are single-phase.

Sample-dependence in κ and τ measurements

We performed experiments on three different α -RuCl₃ crystals, which we have labelled in time order. Figure 1 of the main text shows our results for $\kappa(T)$ for Samples 1, 2, and 3 at selected field values. We reiterate that the primary features of $\kappa(T)$, namely T_C , H_{\min} , the peak positions, and the trends in peak heights, are little changed between samples. However, it is clear that quantitative details of our measurements do differ between samples, particularly the heights of the peak features for H both below and above H_{\min} in Fig. 1(a) and the widths and centers of the low- T ($T < 10$ K) peaks of Samples 1 and 2, which are compared in Figs. 1(b) and 1(c).

For completeness, we show in Fig. S1 the H -dependence of κ for Samples 1 and 2; $\kappa(H)$ of Sample 1 is shown in scaled form in Fig. 2(b) of the main text, and here we compare it directly with Sample 2. The relative changes in κ induced by the applied field are discernibly smaller for Sample 2 than for Sample 1. However, as

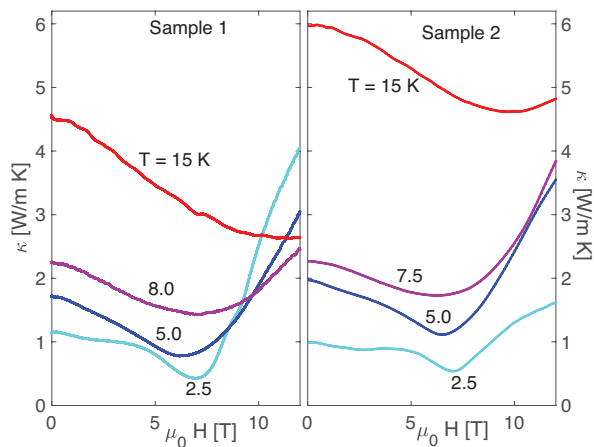


FIG. S1: Thermal conductivity, $\kappa(H)$, of (a) Sample 1 and (b) Sample 2, shown at selected values of T .

above the overall characteristics of the H -dependence, namely the pronounced minima at $H = H_{\min} \approx 7$ T for $T < T_C$, the rapid increase at $H > H_{\min}$, and the movement of H_{\min} to higher fields with increasing T , are consistent across the different samples. We state here that we do not have comparable measurements for Sample 3. Regrettably, because this appears from Fig. 1(a) of the main text to be our highest-quality crystal, we suffered a sample breakage after our first measurements with Sample 3, and this is why we have no data comparable either with Fig. S1 or with Figs. 1(b) and 1(c).

By contrast, the samples used in our magnetic torque measurements showed very consistent results. These measurements are made with much smaller crystals and were repeated three separate times in the course of 9 months. The size of the samples used for torque measurements is typically 100–200 μm , which is more than 10 times smaller in linear dimension than those used for the measurement of κ .

Sources of sample-dependence

The variations we observe in the low-temperature thermal conductivity indicate a non-negligible role for different extrinsic factors, including impurities, defects, stacking faults, and magnetic domains. In one well-documented example, the authors of Ref. [27] showed that limited physical working of $\alpha\text{-RuCl}_3$ can act to alter the c -axis stacking arrangement of the honeycomb layers, which has a direct effect on the magnetic transition temperature. Although our pristine crystals were nearly free from stacking faults, and from the formation of associated domains, it is quite plausible that different mechanical forces were applied on the different samples during their preparation for the κ measurements. However,

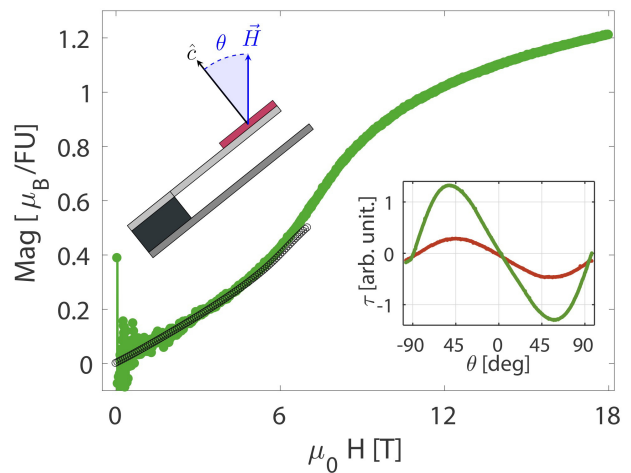


FIG. S2: Torque magnetization, $M_\tau = \tau/H$, measured at $T = 1.5$ K in the geometry shown in the left inset with $\theta \simeq 87^\circ$. Results for M_τ are scaled to match magnetization data measured up to $\mu_0 H = 7$ T with a SQUID magnetometer, which are shown as black circles. Right inset: τ as a function of θ at fixed H . The sample magnetization is expected to remain largely within the ab plane over most of the range of θ .

we were not able to find any correlations between the sample-dependent thermal conductivity and other basic characterization results.

Turning to the other extrinsic sources for quantitative differences, although our measurements were performed over an extended period we did not observe significant effects from sample aging; while we tried to minimize extended exposure to air where possible, these effects would include air-sensitivity and surface degradation. As a result, we did not record much sample variation of the dc susceptibility. However, we do infer a significant difference between samples in the density of magnetic domains and defects, two quantities to which the thermal conductivity is considerably more sensitive than are bulk probes (dc susceptibility and also specific heat). In addition to the c -axis stacking, other causes of domain formation include the threefold degeneracy of the zig-zag ordered structure and twinning in the monoclinic crystal structure. The smaller sample-dependence observed in the magnetic torque suggests a relatively smaller sensitivity of this quantity to the presence of domains.

III. Magnetic torque measured by out-of-plane field rotation

The strong magnetic anisotropy between the ab -plane and the c -axis makes it possible to recover a reliable estimate of the in-plane magnetization from measurements of the torque. Because $\vec{\tau} = \mu_0 V \vec{M} \times \vec{H}$, the magnitude

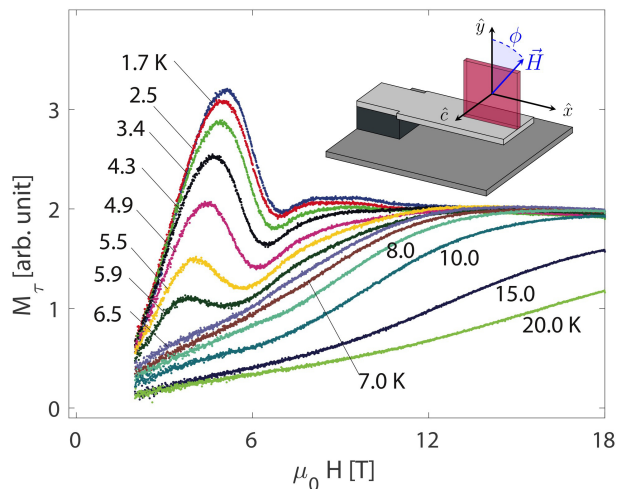


FIG. S3: Torque magnetization, $M_\tau(H)$, measured with H applied in the ab -plane. Inset: schematic representation of measurement geometry. Field sweeps were performed at $\phi = -69^\circ \pm 2^\circ$, which is approximately 5° away from the angle where $\tau \rightarrow 0$.

of the torque is given by $MH \sin \theta'$, where θ' is the angle between \vec{M} and \vec{H} . In the geometry shown in the left inset of Fig. S2, the easy-plane magnetic anisotropy means that $\theta' \rightarrow 0$ when $\theta \rightarrow 90^\circ$ and therefore $|\vec{\tau}| \rightarrow 0$. Similarly, when $\theta \rightarrow 0$, i.e. H is aligned to the hard axis, the component of \vec{M} aligned to the field is almost zero and the measured $\tau \rightarrow 0$. This is illustrated in the θ -

dependence of τ at fixed H , shown in the right inset of Fig. S2. The H -dependence of M_τ deduced from torque measurements performed at $\theta = 87^\circ \pm 2^\circ$, where 2° is the experimental uncertainty in the out-of-plane angle, gives a good approximation to the averaged in-plane magnetization. The magnitude of M_τ is calibrated by matching to the magnetization measured by a SQUID magnetometer. Our results (Fig. S2) are fully consistent with the bulk magnetization reported in Ref. [29].

SIII. Torque magnetization measured by in-plane field rotation

Figure S3 shows the torque magnetization, $M_\tau = \tau(H)/H$, obtained by ϕ rotation (inset). These data display directly the information shown by the color contours in Fig. 4 of the main text and the corresponding data for $\tau(H)$ are shown in Fig. 3. We reiterate that non-monotonic H -dependence appears only for $H < H_{\min} \simeq 7$ T, beyond which the data converge to a constant value of M_τ if $T < 10$ K. Further increase of T causes the magnitude of M_τ to drop significantly. Because the out-of-plane magnetic anisotropy is poorly understood, unlike the case of θ rotation (Sec. SII) the decomposition of M_τ from ϕ rotation into two or more orthogonal components is not trivial. The torque data used here were measured at $\phi \simeq -69^\circ$ (inset, Fig. 3, main text), a position in which M is very well aligned with H .